Available online at www.sciencedirect.com
SCIENCE DIRECT
Journal of Molecular Structure 753 (2005) 53–60
Journal of MOLECULAR STRUCTURE
www.elsevier.com/locate/molstruc

Structure in solid state of 3,3′-diindolylmethane derivatives, potent cytotoxic agents against human tumor cells, followed X-ray diffraction and ^{13}C CP/MAS NMR analyses

Dorota Maciejewska[a,*], Irena Wolska[b], Maria Niemyjska[a], Paweł Żero[a]

[a]*Department of Organic Chemistry, Faculty of Pharmacy, Medical University of Warsaw, 1 Banacha Str, 02 097 Warsaw, Poland*
[b]*Department of Crystallography, Faculty of Chemistry, Adam Mickiewicz University, 6 Grunwaldzka Str, 60 780 Poznań, Poland*

Received 4 April 2005; revised 20 May 2005; accepted 24 May 2005
Available online 21 July 2005

Abstract

The 5,5′-disubstituted-3,3′-diindolylmethanes **1**, **2** have been prepared and their structure was analyzed by X-ray and NMR techniques. The X-ray diffraction studies revealed interesting C–H$\cdots\pi$ intermolecular interactions which may play role in characterization of their biological features. In ^{1}H and ^{13}C NMR spectra in solution and in ^{13}C CPMAS NMR spectra in solid state only a single pattern of signals was observed. Both compounds reduce the growth of MCF7 (breast), NCI–H460 (lung), and SF-268 (NCS) cells dramatically.

Keywords: 5,5′-disubstituted-3,3′-diindolylmethanes; X-ray data; Analysis of ^{1}H; ^{13}C NMR spectra in solution and in solid state; Cytotoxicity

1. Introduction

Clinical management of human reproductive organ cancers still needs new chemotherapeutics. Recently, many efforts have been made to define antiproliferative signaling pathway of indole-3-carbinol (a natural component of cruciferous vegetables) and its major indole metabolite 3,3′-diindolylmethane [1–7]. Although 3,3′-diindolylmethane greatly reduces the incidence of spontaneous and carcinogen induced mammary tumor formation [8–10], it also exhibits adverse promoting activity in certain test protocol [11,12]. Therefore we decided to search for new potent chemotherapeutics among 3,3′-diindolylmethane derivatives. Moreover, our X-ray studies of 5,5′-dimethoxy-3,3′-methanediyl-*bis*-indole [13] revealed its 'butterfly' conformation, which is analogous to the one proposed earlier for inhibitors of HIV-1 reverse transcriptase, sharing the mode of action of nevirapine [14]. We are hopeful that structural analysis of the title compounds in solid state can provide useful information for further development of our work. It is clear that determination the nature of the interaction of drug with its macromolecular target is most informative in drug design process, however examinations just the structure of the designed compounds could be essential for obtaining experimental parameters, which can become descriptors in planned structure-activity studies.

In the present work we report synthesis, the single crystal X-ray diffraction measurements, the analysis of ^{1}H, ^{13}C NMR spectra in solution and ^{13}C CPMAS NMR spectra in solid state, as well as cytotoxicity of 3,3′-diindolylmethane derivatives **1**, **2** (Fig. 1).

2. Experimental

2.1. Synthesis

Melting points were determined with a Digital Melting Point Apparatus 9001 and are uncorrected. All reported elemental analyses were averaged from two independent determinations. Prefabricated silica gel sheets (Merck Kieselgel 60 F_{254}) were used for TLC and Merck Kieselgel 60 was used for column chromatography. Reagents were obtained from commercial sources.

* Corresponding author. *Corresponding author. Tel.: +48 22 572 0643; fax: +48 22 572 0643.
E-mail address: domac@farm.amwaw.edu.pl (D. Maciejewska).

0022-2860/$ - see front matter © 2005 Elsevier B.V. All rights reserved.
doi:10.1016/j.molstruc.2005.05.035

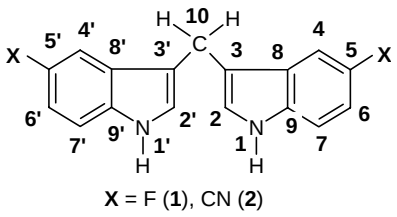

Fig. 1. Chemical formulas and atom numbering of 5,5′-difluoro-3,3′-methanediyl-*bis*-indole **1** and 5,5′-dicyano-3,3′-methanediyl-*bis*-indole **2**.

Compounds **1** and **2** were synthesized from the corresponding indoles and formaldehyde in a one-step process according to the reported procedure [15, 16] with slight modifications. The reaction and purification processes were performed out of the light. It was not necessary to keep the reaction vessel under nitrogen to obtain a sufficient yield (28–37%). The reactants were solved in water/ethanol solution, vol. 225:60 ml with 2.85 ml of 0.5 M sulfuric acid. The crude precipitate of **1** was separated chromatographically on silica gel with hexane/dichloromethane, 1:6. The precipitate of **2** was crystallized from diluted ethanol (water:ethanol = 1:1). The melting points, elemental analyses, and ^{1}H and ^{13}C NMR data in solution are given below. The notation used in the NMR assignments is given in Fig. 1. The other method of synthesis of 5,5′-difluoro-3,3′-methanediyl-*bis*-indole 1, as well as its antitumorigenic activity were reported [17]. In our opinion, the physicochemical characterization of **1** is not sufficient, and we have a feeling of uncertainty, if the compound examined by authors is identical with this synthesized by us.

5,5′-*Difluoro*-3,3′-*methanediyl-bis-indole* **1** –37% yield. M. p. 144.5–145.5 °C.-IR (KBr):$\tilde{\nu}$ = 3470(N–H), 3120-3040, 2970, 2850, 1620, 1580, 1480, 1440, 1430, 1280 cm^{-1}.-^{1}H NMR (500.13 MHz, $CDCl_3$): δ = 4.127 (s, 2 H, CH_2), 6.921 (td, J = 9.5, 2.5 Hz, 2H, 6-H, 6′-H), 6.984 (dd, J = 2, 1 Hz, 2 H, 2-H, 2′-H), 7.202 (dd, J = 9.5, 2.5 Hz, 2 H, 4-H, 4′-H), 7.245 (dd, J = 9.5, 4.5 Hz, 2 H, 7-H, 7′-H), 7.885 (broad s, 2 H, 1-NH, 1′-NH).-^{13}C NMR (125.68 MHz, $CDCl_3$): δ = 21.29 (C-10), 104.07 (d, J = 23.3 Hz, C-4, C-4′) , 110.32 (d, J = 26.4 Hz, C-6, C-6′), 111.66 (d, J = 9.1 Hz, C-7, C-7′), 115.41 (d, J = 4.5 Hz, C-3, C-3′), 123.93 (C-2, C-2′), 127.80 (d, J = 9.5 Hz, C-8, C-8′), 132.96 (C-9, C-9′), 157.63 (d, J = 232.8 Hz, C-5, C-5′) ppm.-$C_{17}H_{12}N_2F_2$ (282.28): calcd. C 72.33, H 4.29, N 9.92; found C 70.82, H 4.00, N 9.46.

5,5′-*Dicyano*-3,3′-*methanediyl-bis-indole* **2** –28% yield. M. p. 232.0–232.5 °C. decomp. IR (nujol) :$\tilde{\nu}$ = 3340(N–H), 3050, 2800, 2240 (C≡N), 1630, 1470, 1430, 1220 cm^{-1}.-^{1}H NMR (500.13 MHz, $(CD_3)_2CO$): δ = 4.351 (s, 2 H, CH_2), 7.381 (dd, J = 8.5, 1.54 Hz, 2 H, 6-H, 6′-H), 7.481 (dd, J = 3, 1.5 Hz, 2H, 2-H, 2′-H), 7.564 (dd, J = 8.5, 0.5 Hz, 2 H, 7-H, 7′-H), 8.037 (dd, J = 1.5, 0.8 Hz, 2 H, 4-H, 4′-H), 10.612 (broad s, 2 H, 1-NH, 1′-NH).-^{13}C NMR (125.68 MHz, $(CD_3)_2CO$): δ = 21.37 (C-10), 102.36 (C-5, C-5′), 113.43 (C-7, C-7′), 116.39 (C-3, C-3′), 121.34 (C≡N), 124.81 (C-6, C-6′), 125.29 (C-4, C-4′), 126.32 (C-2, C-2′), 128.25 (C-8, C-8′), 139.49 (C-9, C-9′), ppm.-$C_{19}H_{12}N_4$ (296.32): calcd. C 77.01, H 4.08, N 18.91; found C 76.95, H 4.15, N 19.00.

2.2. Crystallography

The crystals of **1** and **2** suitable for X-ray analysis were grown from methanol solution by slow evaporation. Diffraction data were collected on an Oxford Diffraction KM4CCD diffractometer [18] at 150 K, using graphite-monochromated Mo Kα radiation. A total of 532 and 588 frames were measured in four separate runs for **1** and **2**, respectively. The ω-scan was used with a step of 0.75°, two reference frames were measured after every 50 frames, they did not show any systematic changes either in peaks positions or in their intensities. The unit cell parameters were determined by least-squares treatment of setting angles of 1768 and 7139 highest-intensity reflections chosen from the whole experiment for **1** and **2**, respectively. Intensity data were corrected for the Lorentz and polarization effects [19]. The structures were solved by direct methods with the SHELXS-97 program [20] and refined with full-matrix least-squares by the SHELXL-97 program [21]. The function $\sum w(|F_o|^2 - |F_c|^2)^2$ was minimized with $w^{-1} = [\sigma^2(F_o)^2 + (0.0170P)^2]$ for **1** and $w^{-1} = [\sigma^2(F_o)^2 + (0.0574P)^2 + 0.2218P]$ for **2**, where $P = (F_o^2 + 2F_c^2)/3$. All non-hydrogen atoms were refined anisotropically, positions of hydrogen atoms were generated geometrically and their positional and isotropic displacement parameters were refined.

2.3. NMR spectra

^{1}H NMR and ^{13}C NMR spectra in solutions were recorded with a Varian Unity plus-500, and standard Varian software was employed.

The solid state ^{13}C CP/MAS NMR spectra were measured using a Bruker Avance DM×400. Powdered samples were spun at 8 kHz. Contact time of 7 ms, repetition time of 20 s, and spectral width of 24 kHz were used for accumulation of 2,500 scans. Chemical shifts δ [ppm] were references to TMS.

2.4. Molecular modeling details

Crystallographic atom coordinates were used for computation of shielding constants σ [ppm] of ^{13}C atoms to assign the resonances in solid-state NMR spectra. We have employed the DFT method with B3LYP/6-31(d,p) hybrid functional using the CHF-GIAO approach [22].

2.5. Cytotoxicity against three cell lines

The *in vitro* cell line screening utilizing three different human tumor cell lines consisting of the MCF7 (breast), NCI-H460 (lung), and SF-268 (CNS) was carried out in National Institute of Health, Bethesda, USA. The results are reported as the percentage of growth of the treated cells when compared with the untreated control cells [23]. Additional information details concerning the NCI's drug discovery and development program are available at web site http://dtp.nci.nih.gov.

3. Results and discussion

3.1. NMR spectra

The ^{1}H and ^{13}C chemical shift δ [ppm] and coupling constants J [Hz} in $CDCl_3$ for **1** and in $(CD_3)_2CO$ for **2** are given in Experimental part 2.1. The assignments were based on heteronuclear correlation ^{1}H–^{13}C experiments. We have observed a standard pattern of signals, i.e. the number of peaks was equal to the number of chemically distinct sites in the molecules. This could indicate that no steric hindrance occurs in solution, when indole rings rotate around the methylene linker. The protons of the NH groups in indole rings are strongly deshielded and give the resonances above 8 ppm. We have observed additional splittings of NMR signals in **1** resulting from the presence of F atoms at C5 and C5′ positions. The J_{C-F} coupling constants through one, two three and four bonds are equal to 233, 25, 9, 5 Hz, respectively.

The ^{13}C CP/MAS NMR spectroscopy in solid state is a complementary tool to X-ray diffraction method. Of special interest is the application of solid state NMR to the investigation of polymorphism and dynamic events of biologically active substances in solid state. The ^{13}C

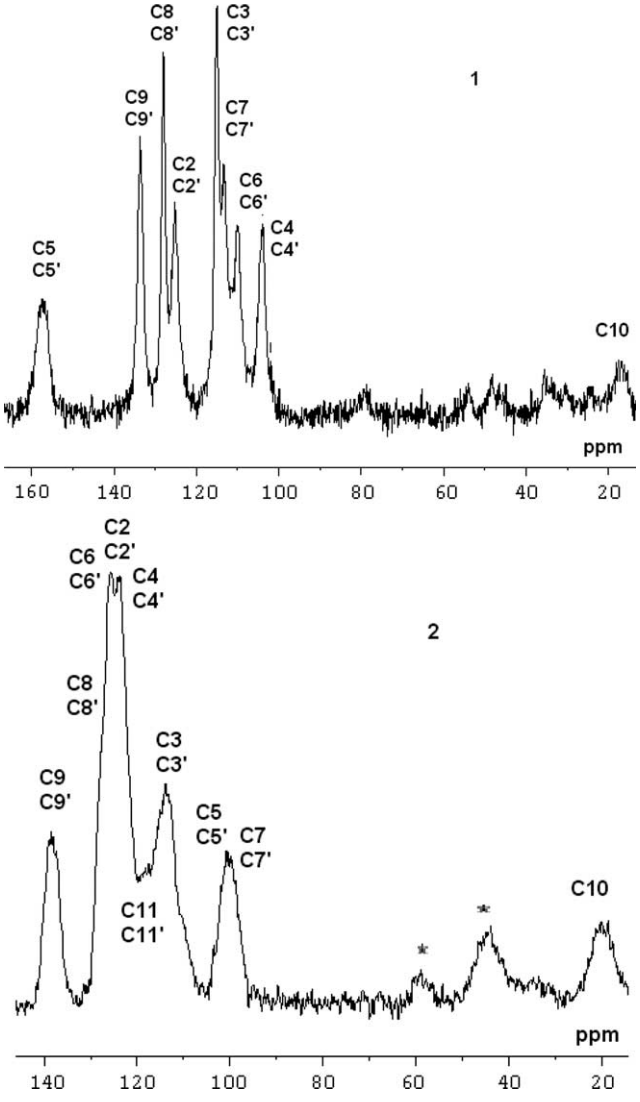

Fig. 2. The ^{13}C CP/MAS NMR spectra of 5,5′-difluoro-3,3′-methanediyl-*bis*-indole **1** and 5,5′-dicyano-3,3′-methanediyl-*bis*-indole **2** in solid state. Sidebands are marked with an asterix.

Table 1
Assignments of resonances in ^{13}C CP/MAS NMR spectra of compounds **1** and **2**. chemical shifts of ^{13}C in solid state, δ [ppm]

comp	chemical shifts of ^{13}C in solid state, δ [ppm]									
1	C2;C2′	C3;C3′	C4;C4′	C5;C5′	C6;C6′	C7;C7′	C8;C8′	C9;C9′	C1017.5	
	125.3	115.0	103.8	157.4	110.0	113.4	128.0	133.6		
2	C2;C2′	C3;C3′	C4;C4′	C5;C5′	C6;C6′	C7;C7′	C8;C8′	C9;C9′	C10	C≡N
	124.1	113.9	123.6	110.8	125.6	99.5	125.6	138.5	18.9	117.8

CP/MAS NMR spectra of **1** and **2** are shown in Fig. 2 and the most probable assignments of signals are given in Table 1. Surprisingly, the number of resonances in both spectra was consistent with solution spectra (or even less), contrary to our findings for 5,5′-dimethoxy-3,3′-methanediyl-bis-indole, where we observed double signals of C atoms [13]. Then we decided to compute the shielding constants for appropriate assignment of resonances. The calculated shielding constants, based on crystallographic coordinates, of carbon atoms in 5,5′-difluoro-3,3′-methanediyl-bis-indole **1** are pairwise equal, which explains the observed pattern of resonances. It is not the case of 5,5′-dicyano-3,3′-methanediyl-bis-indole **2**. The signals are poorly resolved. Some splitting could be explained in terms of ^{13}C-^{14}N residual dipolar coupling, but not all. The calculated shielding constants for relevant carbon atoms in both indole rings differ insignificantly from each other; it results in broad, overlapped resonances.

3.2. X-ray diffraction study

The crystal and molecular structures of **1** and **2** were determined by single crystal X-ray diffraction. The -crystallographic data, together with data collection and structure refinement details are listed in Table 2. Selected bond lengths, bond angles and torsion angles are listed in Table 3 and hydrogen bonding parameters in Table 4. Additional crystallographic data have been deposited with the Cambridge Crystallographic Data Centre as supplementary publications No CCDC 272 415 for **1**, and 272 416 for **2**. The displacement ellipsoid representation of the

Table 2
Crystal data, data collection and structure refinement for compounds **1** and **2**

Compound	**1**	**2**
Empirical formula	$C_{17}H_{12}F_2N_2$	$C_{19}H_{12}N_4$
Formula weight	282.29	296.33
T (K)	150(2)	150(2)
Wavelength (Å)	0.71073	0.71073
Crystal system, space group	orthorhombic, *I ba2*	monoclinic, *P* 2_1/c
Unit cell dimensions		
a (Å)	11.611(1)	11.543(2)
b (Å)	13.005(1)	13.546(3)
c (Å)	8.672(1)	9.633(2)
β (°)		90.63(3)
Volume (Å^3)	1309.5 (2)	1506.2(5)
Z, D_x (Mg/m^3)	4, 1.432	4, 1.307
μ (mm^{-1})	0.105	0.081
F(000)	584	616
θ range for data collection (°)	5.26–29.34	3.13–29.26
hkl range	$-15 \le h \le 15$	$-15 \le h \le 15$
	$-17 \le k \le 17$	$-18 \le k \le 15$
	$-5 \le 1 \le 11$	$-13 \le 1 \le 13$
Reflections		
Collected	4253	10524
unique (R_{int})	1049 (0.053)	3769 (0.031)
observed ($I > 2\sigma(I)$)	706	3183
Data/restraints/parameters	1049/1/120	3769/0/256
Goodness-of-fit on F^2	0.855	1.089
$R(F)$ ($I > 2\sigma(I)$)	0.0352	0.0388
$wR(F^2)$ (all data)	0.0524	0.1069
Max/min. Δρ (e/Å^3)	0.171/–0.157	0.220/–0.217

Table 3
Selected bond lengths [Å] and angles [deg] and selected torsional angles [deg] for compounds **1** and **2**

	1	**2**
N1–C9	1.373(2)	1.369(1)
N1′–C9′	1.373(2)	1.366(1)
N1–C2	1.373(3)	1.380(1)
N1′–C2′	1.373(3)	1.382(1)
C2–C3	1.358(3)	1.370(1)
C2′–C3′	1.358(3)	1.366(1)
C8–C9	1.413(2)	1.422(1)
C8′–C9′	1.413(2)	1.427(1)
C9–N1–C2	108.9(2)	108.7(1)
C9′–N1′–C2′	108.9(2)	108.8(1)
C3–C10–C3′	114.3(3)	112.7(1)
C8–C3–C10–C3′	78.2(2)	−87.7(1)
C8′–C3′–C10–C3	78.2(2)	−174.8(1)
N1–C2–C3–C10	179.2(2)	−177.8(1)
N1′–C2′–C3′–C10	179.2(2)	−179.2(1)

molecules, together with the atomic numbering scheme, is shown in Fig. 3 (the drawings were performed with a Stereochemical Workstation [24]).

Compound **1** crystallizes in the orthorhombic space group I ba2 with a half of the ordered molecule in the asymmetric unit (the molecule occupies a special position: the C10 atom is located at two-fold axis) and compound **2** crystallizes in the monoclinic space group $P\ 2_1/c$ with a single ordered molecule in the asymmetric unit. The structures consist of two indole systems connected by a common C atom (C10). Bond lengths observed in the molecules are in good agreement with the corresponding distances in the related compounds [13, 25]. X-ray results indicate that studied *bis*-indoles adopt a butterfly conformation (see Fig. 4) similar to that observed for 5,5′-dimethoxy-3,3′-methanediyl-*bis*-indole [13]. The indole fragments are essentially planar to within 0.026(2)Å (for **1**) and 0.021(1)Å (for **2**) with the dihedral angle between their mean planes of 72.98(4)° and 88.53(4)° for **1** and **2**, respectively. However the molecular structures of **1** and **2** differ in the arrangement of these fragments (the appropriate torsion angles are given in Table 3). The other non-H atoms are nearly coplanar with that two-ring framework. The disposition of the C≡N groups in **2** with respect to the indole fragments can be described by the torsion angles C4–C5–C11–N12 of –171(3)° and C4′–C5′–C11′–N12′ of 35(3)°. So, these results indicate that there are insignificant differences between the structures of these fragments. This may be the reason why the calculated shielding constants for relevant carbon atoms in both indole rings of **2** are slightly different.

Table 4
Hydrogen-bonding geometry [Å and deg.] for compounds **1** and **2**

D–H···A	d(D–H)	d(H· ···A)	d(D····A)	<(DHA)
Compound 1				
N1–H1···F^{i}	0.86(2)	2.35(2)	3.055(2)	139(2)
C7–H7···F^{i}	0.95(2)	2.64(2)	3.320(3)	129(2)
N1–H1···^{ii}	0.86(2)	2.49(2)	3.236(2)	147(2)
C6–H6···Cg^{iii}	0.95(2)	2.75(2)	3.593(2)	148(2)
Compound 2				
N1–H1···N12′^{i}	0.91(1)	2.16(1)	2.949(1)	143(1)
N1′–H1′···N12^{ii}	0.90(2)	2.15(2)	2.984(1)	153(1)
C6–H6···N12′^{iii}	1.00(1)	2.54(1)	3.532(2)	172(1)
C7–H7···N12^{iv}	0.99(1)	2.55(2)	3.398(2)	144(1)
C7′–H7′···Cg^{v}	0.97(2)	2.47(2)	3.430(2)	171(2)

Cg represents the centroid of five-membered ring of the indole;
symmetry codes: (i) 0.5+*x*, 0.5−*y*, *z*; (ii) 0.5−*x*, −0.5+*y*, z; (iii) 0.5−*x*, 0.5−*y*, −0.5+*z*

Cg represents the centroid of five-membered ring (N1/C2/C3/C8/C9) of the indole; symmetry codes: (i) 1−*x*, 0.5+*y*, −0.5−*z*; (ii) 2−*x*, 0.5+*y*, −0.5−*z*; (iii) 1+*x*, *y*, 1+*z*; (iv) 2−*x*, 0.5+*y*, 0.5−*z*; (v) *x*, *y*, −1+*z*.

In the crystals of **1** and **2** the packing of the molecules is stabilized by different weak intermolecular contacts. The geometric parameters of all hydrogen bonds are given in Table 4. The crystal structure of **1** is built of folded layers perpendicular to the *c* axis (Fig. 4). Cohesion between these layers results from the C−H···π intermolecular interactions. Within the layer the molecules are linked by N−H···F and C−H···F hydrogen bonds (Fig. 5, Table 4). In the crystal of **2**, there is a three-dimensional network of N−H···N, C−H···N and C−H···π interactions (Fig. 6, Table 4). The molecules are connected *via* N−H···N intermolecular hydrogen bonds along the two-fold screw *b* axis. Additionally the C−H···π interactions link the molecules to infinite chains along the *c* axis. The N12 and N12′ atoms are also involved in weak intermolecular C−H···N interactions, which results from the crystal packing of the molecules.

So, we have observed the interactions between the CH groups and the π-electron system of indole rings. Analogous N−H···π contacts were observed for 5,5′-dimethoxy-3,3′-methanediyl-*bis*-indole [13], other indole derivatives [26, 27] and for globular proteins [28].

3.3. Primary anticancer assay

5,5′-Difluoro-3,3′-methanediyl-*bis*-indole **1** and 5,5′-dicyano-3,3′-methanediyl-*bis*-indole **2** were examined against the MCF7 (breast), NCI-H460 (lung), and SF-268 (CNS) tumor cell lines. The results are reported as the percentage of growth of the treated cells when compared with untreated control cells. The derivative **1** at conc. 1.10^{-4} M reduces the growth of MCF7, NCI-H460, and SF-268 cell lines to 1, 0, and 2 percent, whereas the derivative **2** at conc. 5.10^{-5} M- to 4, 1, and 9 percent, respectively. Both compounds are highly cytotoxic *in vitro* against those tumor lines.

4. Conclusions

X-ray analysis of 5,5′-difluoro-3,3′-methanediyl-*bis*-indole **1** and 5,5′-dicyano-3,3′-methanediyl-*bis*-indole **2**

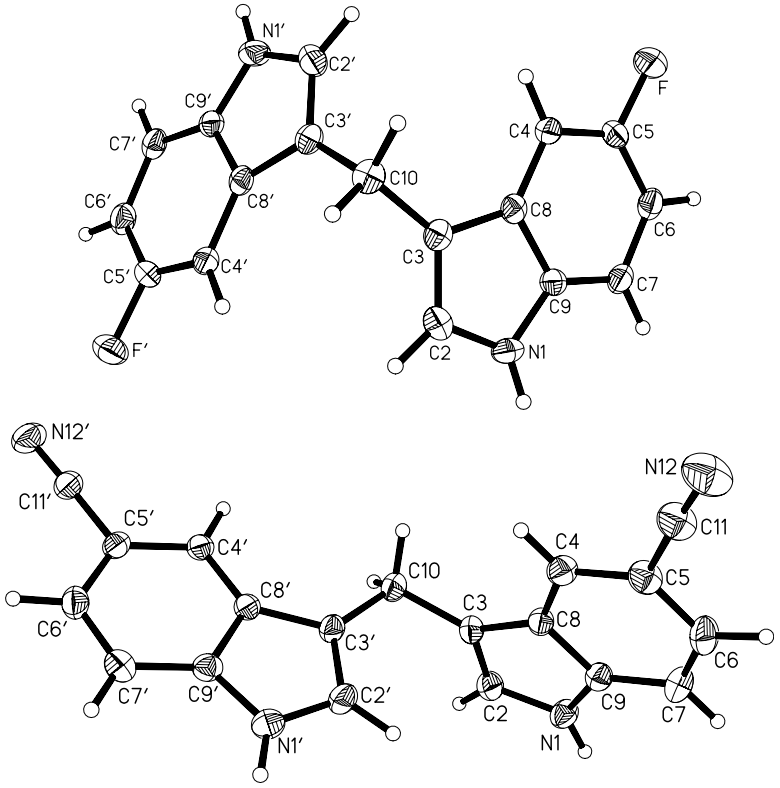

Fig. 3. Molecular structure of **1** and **2** with 50% probability displacement ellipsoids and atom-numbering scheme.

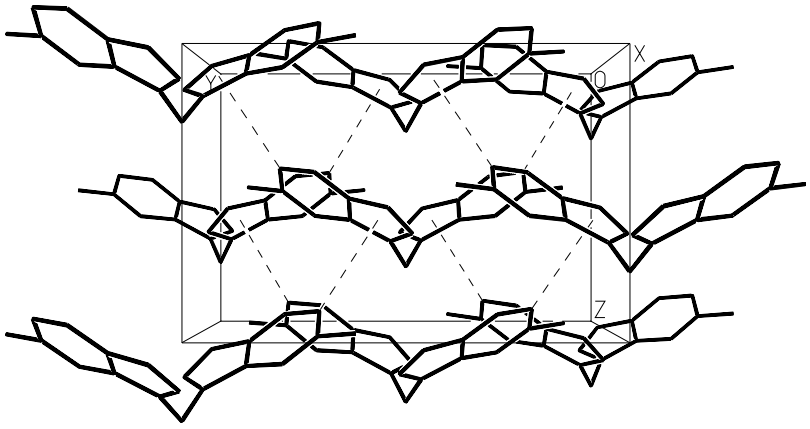

Fig. 4. Projection of the crystal structure of **1** along the *a* axis with C−H···π intermolecular hydrogen-bonding interactions. H atoms are omitted for clarity.

revealed interesting interactions between the CH groups and the π-electron system of indole rings. They adopt a butterfly conformation which may have a functional role in their biological features. Their cytotoxicity indicates that they could be interesting as potential antitumoral chemotherapeutics.

According to ^{1}H and ^{13}C NMR data no hindered rotation phenomena are observed in solution. In ^{13}C CPMAS NMR spectra only single pattern of signals was observed.

Acknowledgements

The computational results discussed in this work were obtained using the resources of Interdisciplinary Centre for Mathematical and Computational Modelling (ICM) Warsaw University.

References

[1] W. Wattenberg, W.D. Loub, Cancer Res. 38 (1978) 1410.

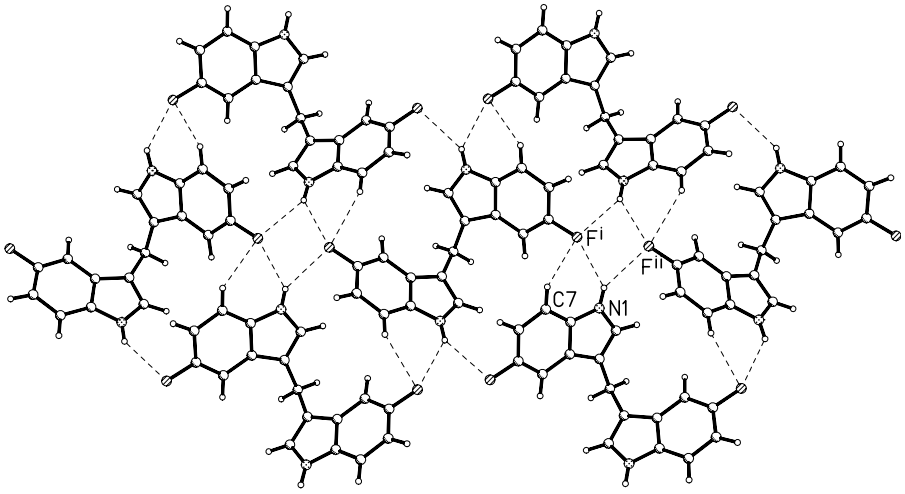

Fig. 5. A view showing the interconnections within a layer of 1. Dashed lines indicate hydrogen bonds. The symmetry codes are the same as those given in Table 4.

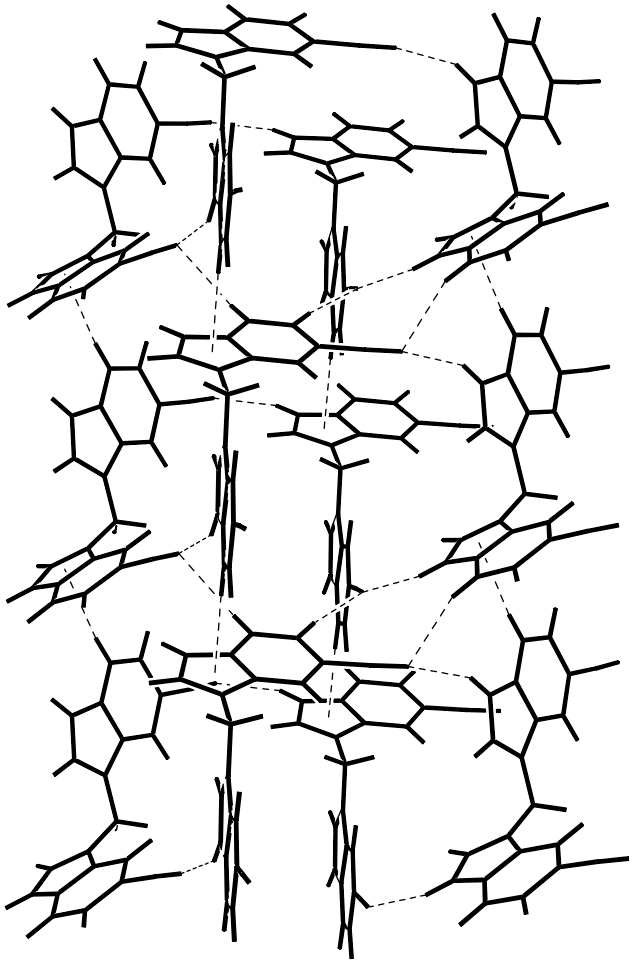

Fig. 6. A fragment of the crystal structure of 2.

[2] C.A. Bradfield, L.F. Bjeldanes, Food Chem. Toxicol. 22 (1984) 346.
[3] H.L. Bradlow, D.W. Sepkovic, N.T. Telang, M.P. Osborne, Ann. N.Y. Acad. Sci. 768 (1995) 180.
[4] I. Chen, S. Safe, L. Bjeldanes, Biochem. Pharmacol. 51 (1996) 1096.
[5] O. Vang, M.B. Jensen, H. Autrup, Carcinogenesis 11 (1990) 1259.
[6] C. Hong, H.A. Kim, G.L. Firestone, L. Bjeldanes, Carcinogenesis 23 (2002) 1297.
[7] G.L. Firestone, L.F. Bjeldanes, J. Nutr. 133 (2003) 2448S.
[8] C.J. Grubbs, V.E. Steele, T. Casebolt, M.M. Juliana, I. Eto, L.M. Whitaker, et al., Anticancer Res. 15 (1995) 709.
[9] S.R. Chinni, Y. Li, S. Upadhyay, P.K. Koppolu, F.H. Sarkar, Oncogene 20 (2001) 2927.
[10] D.Z. Chen, M. Qi, K.J. Auborn, T.H. Carter, J. Nutr. 131 (2001) 3294.
[11] R.H. Dashwood, A.T. Fong, D.E. Williams, J.D. Hendricks, G.S. Baley, Cancer Res. 51 (1991) 2362.
[12] D.J. Kim, B.S. Han, B. Ahn, R. Hasegawa, T. Shirai, N. Ito, H. Tsuda, Carcinogenesis 18 (1997) 377.
[13] D. Maciejewska, M. Niemyjska, I. Wolska, M. Włostowski, M. Rasztawicka, Z. Naturforsch. 59b (2004) 1137.
[14] S. Hannongbua, S. Prasithichokekul, P. Pungpo, J. Comput Aided, Mol. Des. 15 (2001) 997.
[15] J. Thessing, Chem. Ber. 31 (1954) 692.
[16] S. Földeal, J. Czombas, B. Matkowics, Acta Phys. Chem. 11 (1965) 115.
[17] A. McDougal, M.S. Gupta, K. Ramamoorthy, G. Sun, S.H. Safe, Cancer Letters 151 (2000) 169.
[18] Oxford Diffraction Poland, CrysAlisCCD, CCD data collection GUI, version 1.171, 2003.
[19] Oxford Diffraction Poland, CrysAlisRED, CCD data reduction GUI, version 1.171, 2003.
[20] G.M. Sheldrick, Acta Crystallogr. A46 (1990) 467.
[21] G.M. Sheldrick, SHELXL97, Program for the Refinement of Crystal Structures, University of Göttingen, Germany, 1997.
[22] M.J. Frisch, G.W. Trucks, H.B. Schlegel, G.E. Scuseria, M.A. Robb, J.R. Cheeseman, V.G. Zakrzewski, J. A. Montgomery, Jr., R. E. Stratmann, J. C. Burant, S. Dapprich, J. M. Millam, A. D. Daniels, K. N. Kudin, M. C. Strain, O. Farkas, J. Tomasi, V. Barone, M. Cossi, R. Cammi, B. Mennucci, C. Pomelli, C. Adamo, S. Clifford, J. Ochterski, G.A. Petersson, P.Y. Ayala, Q. Cui, K. Morokuma, D.K. Malick, A.D. Rabuck, K. Raghavachari, J.B. Foresman, J. Cioslowski, J.V. Ortiz, -A.G. Baboul, B.B. Stefanov, G. Liu,A. Liashenko, P. Piskorz, I. Komaromi, R. Gomperts, R.L. Martin, D.J. Fox, T. Keith, M.A.

Al-Laham, C.Y. Peng, A. Nanayakkara, C. Gonzalez, M. Challacombe, P.M.W. Gill, B. Johnson, W. Chen, M.W. Wong, J.L. Andres, C. Gonzalez, M. Head-Gordon, E.S. Replogle, and J.A. Pople, Gaussian 98, Revision A.7, Gaussian, Inc., Pittsburgh PA, 1998

[23] M.R. Boyd, K.D. Pauli, Drug Develop. Res. 34 (1995) 91.

[24] Stereochemical Workstation Operation Manual. Release 3.4. Siemens Analytical X-ray Instruments Inc., Madison, Wisconsin, USA, 1989.

[25] F.H. Allen, Acta Crystallogr. B58 (2002) 380 ; CSD, Version 5.25 of November 2003 and three updates.

[26] R. Krishna, D. Velmurugan, G. Babu, P.T. Perumal, Acta Crystallogr. C55 (1999) 75.

[27] R. Krishna, D. Velmurugan, S. Shanmuga Sundara, Acta Crystallogr. C55 (1999) IUC9900084.

[28] M. Crisma, F. Formaggio, G. Valle, C. Toniolo, M. Saviano, R. Lacovino, L. Zaccaro, E. Benedetti, Biopolymers 42 (1997) 1.